Proceedings of the International Conference on Heat Exchanger Fouling and Cleaning - 2024 (Peer-reviewed)
April 21–26, 2024, Lisbon, Portugal; Editors: H.U. Zettler and E.M. Ishiyama

THE DYNAMIC FOULING BEHAVIOR OF WHEY PROTEINS THROUGHOUT A PLATE HEAT EXCHANGER: UTILIZING A VALIDATED KINETIC FOULING MODEL

J. Zha[1,2], L. Bouvier[1], J. Xiao[2,*], H. Dallagi[1] and G. Delaplace[1,*]
[1] UMET – Unité Matériaux et Transformations, UMR 8207 (Univ. Lille, CNRS, INRAE, Centrale Lille), 59000 Lille, France, guillaume.delaplace@inrae.fr
[2] School of Chemical and Environmental Engineering, College of Chemistry, Chemical Engineering and Materials Science, Soochow University, Suzhou, Jiangsu Province 215123 China, jie.xiao@suda.edu.cn

ABSTRACT

In dairy processing, β-lactoglobulin (BLG), the predominant component of whey protein solutions, significantly contributes to fouling in plate heat exchangers (PHEs), which are involved in milk derivative production. However, observing the formation and growth of fouling under experimental conditions within closed PHEs presents challenges. As a result, simulation has emerged as an alternative approach that has attracted considerable attention. A validated simulation model is essential for achieving a more accurate description and prediction of the fouling behavior of whey solutions. In this work, a 2D dynamic model for PHEs was proposed based on the measured kinetics of denaturation and deposition obtained by experiments. In this 2D dynamic model, the entire PHE is simulated to account for real temperature variations of the product along the PHE path. This innovative approach not only reflects the dynamic interplay between fouling and bulk liquid but also serves as a reliable tool for predicting milk fouling. It promises to enhance our understanding of milk fouling mechanisms, potentially transforming practices in the dairy industry by enabling more effective fouling management strategies.

INTRODUCTION

Pasteurization has been proven to be a convenient and effective way to realize microbiological harmlessness and extend shelf life [1]. However, during heat treatment, fouling is a problem in the dairy industry. The existence of unwanted fouling deposits can lead to many issues, such as limiting heat transfer efficiency, enhancing the pressure drop, and increasing the possibility of bio-contamination due to insufficient cleaning. The operating costs are therefore increased due to frequent shutdowns for cleaning as well as the corresponding use of excessive water and erosive chemicals [1]. According to the literature, approximately 80 % of the total production costs are attributed to fouling [2].

β-Lactoglobulin, the primary component of lactoserum, is known to play a key role in the fouling of whey protein solutions but also in milk fouling, despite not being the majority protein of milk (casein is the majority protein in this case). Previous work revealed that the fouling process of BLG is multistage and is also influenced by calcium [3]. With increasing temperature, the noncovalent bond breaks, and native BLG (N) is converted to an unfolded state; this transformation is reversible when the temperature is below 60 °C [1, 4]. With increasing temperature, the covalent bond breaks, and unfolded BLG (U) is transformed into irreversible aggregated BLG (A). The transformation is represented as $N \rightleftharpoons U \rightarrow A$, which occurs in bulk fluid and is known as the denaturation reaction where calcium acts to catalyze the transformation. Furthermore, fouling deposits (D) are produced based on the surface reaction $U \rightarrow D$, and calcium also facilitates surface reactions.

A large number of experiments and mathematical models have been carried out to explore the mechanism of denaturation and deposition processes in lactoserum solutions, which contain mainly whey protein and calcium, as they are known to be among the most prone to fouling in the dairy industry [5, 6]. Computational fluid dynamics (CFD) models have received increasing amounts of attention because they can provide information inside equipment and reduce experimental costs [7-9]. For modeling denaturation reactions, two models are widely used: the two-step successive model and the one-equation model. The two-step successive model offers a better description of the denaturation process by differentiating two distinct stages ($N \rightarrow U$ and $U \rightarrow A$). However, practical challenges arise in accurately measuring the concentrations of native and unfolded BLG due to technical limitations (both native and unfolded BLG are soluble) [10]. Therefore, in practice, the denaturation process is usually expressed using the equation $S \rightarrow A$, which involves the transformation of soluble BLG to aggregated BLG. Based on the sharp bend in the Arrhenius plot resulting from one equation, the corresponding kinetic parameters are derived for both the unfolding and aggregation regions. Thus,

ISBN: 978-0-9984188-3-4; Published online www.heatexchanger-fouling.com

one equation model is in practice retransformed into a two-stage reaction process. In this way, Bouvier et al. [11] constructed the PHE model and solved the BLG denaturation process within the bulk. The results revealed a close relationship between the predicted unfolded BLG concentration and the distribution of the deposit mass experimentally measured in each channel of the PHE, which further confirmed that unfolded BLG is a key component of fouling deposits.

The concentration of unfolded BLG directly affects the fouling deposition process [12]. While various models have been employed to derive kinetic parameters such as the activation energy E_a and pre-exponential constant k_0, they mainly utilize the deposit kinetic equation from De Jong [13-15]. However, the validity of this kinetic equation for different solutions, which can contain different amounts of calcium, remains uncertain. For example, Petit et al. [3] showed that for similar whey protein solutions with varying levels of calcium, denaturation kinetics were strongly affected by the calcium content. Identification of the denaturation kinetics model of processed whey protein solutions is essential for achieving a more accurate description and prediction of fouling behavior.

To date, CFD simulations incorporating experimentally measured kinetic denaturation parameters have been scarce. A CFD model that considers the complete design and geometry of PHEs is essential for obtaining an in-depth understanding of the fouling mechanism. However, to optimize computational resources, it is necessary to streamline the CFD model without compromising its dynamic nature.

In this work, an innovative 2D dynamic model for PHE fouling was proposed based on a validated kinetic deposition model. This model simulates the entire channels of a PHE (containing heat-treated whey protein solutions), ensuring an accurate representation of temperature variations along the product's path. Computational efforts are concentrated on the process side, where the whey protein solutions are treated, while realistic temperature boundary conditions are implemented on both sides of each plate to mimic the distribution of temperature imposed by the flow of calorific fluid (hot water). The model stands out for its ability to dynamically couple the denaturation kinetics of BLG in bulk fluid with the kinetics of surface reactions, integrating these with comprehensive momentum, mass, and heat transfer mechanisms. This approach not only reduces the computational time but also retains the dynamic essence of the model, offering a practical and efficient tool for predicting and analyzing fouling in PHEs.

MODELING METHODS

Constructed geometry

By incorporating the fouling experiments conducted by Khaldi et al. [10], this study focused on a PHE system featuring five channels of product in a countercurrent configuration (one channel-per-pass) equipped with V7 plates (Alfa Laval Vicarb, Fontanil-Cornillon, France). Fig. 1(a-c) shows the V7 plate used in the experiments and the arrangement of 5 channels. A 2D model was constructed along the plate path indicated by the blue dashed line. The design (see Fig. 1(b-c)) takes into account the complexity of the wavy shape and keeps the heat transfer length the same as that of the actual V7 plate (see Fig. 1(a)).

To simplify the computation, it was decided to only solve transport phenomena within the 5-channel geometry located on the process side (where the dairy derivative flows), while the channel geometry containing the flow of hot water used for heating the milk derivative was excluded. Channel numbers 1-5, shown in red font, are shown in Fig. 1(c) in the following text.

Instead, realistic boundary conditions were applied for the hot wavy wall of the plates (see later initial and boundary conditions).

This model facilitates direct comparison with established research while simplifying the computational domain.

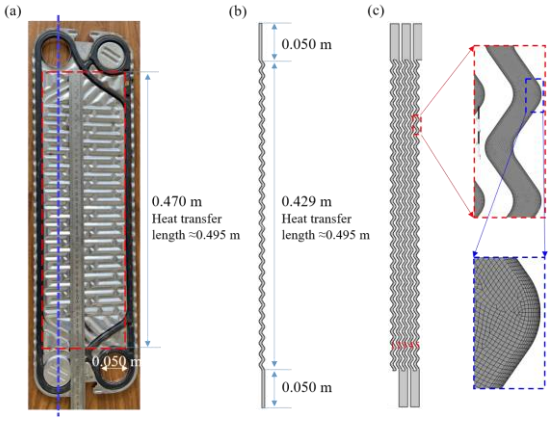

Fig. 1. Geometry of the PHE: (a) one V7 plate of PHE in the experiment, (b) one channel in the simulation, and (c) the overall system with five channels in the simulation, with an enlarged view showing the mesh distribution. In Fig. 1(a), the blue dashed line denotes the location of the cross section for the 2D geometry in the simulation, and the red dashed rectangle denotes the heat exchange region. The channel numbers in Fig. 1(c) are shown in red font.

In this study, we utilized the commercial computational fluid dynamics software ANSYS/Fluent 2022R1 to solve the equations. The simulation was conducted using a two-dimensional modeling geometry, with quadrilateral cells employed for the mesh. The mesh distribution is illustrated in the larger view in Fig. 1(c). The overall

ISBN: 978-0-9984188-3-4; Published online www.heatexchanger-fouling.com

PHE geometry comprises 518313 elements for subsequent calculation and analysis.

Initial and boundary conditions

The initial and boundary conditions are shown in Fig. 2. The boundary conditions of momentum transfer were represented by the velocity inlet v_{in} (m/s), pressure outlet, and wall conditions (as shown in black in Fig. 2). Following preheating, the product enters at an inlet temperature T_{in} and exits from the outlet after heat is exchanged with hot water. The direction of fluid flow is indicated by purple arrows for clarity. The wavy walls represented in Fig. 2 signify the plates in direct thermal contact with the heating medium, hot water. In this study, the real temperature distribution was considered. A specific temperature distribution function of position, identical to that of the experimental conditions, was applied to each wall. As illustrated in the right enlarged view in Fig. 2, in which the 5th channel is taken as an example, the left wall exhibits a temperature distribution of $T_{C5,\ left}$, while the right wall has $T_{C5,\ right}$. For each experiment, the specific temperature distribution function in the PHE was simulated numerically using Sphere software, which was previously developed in the laboratory, as mentioned in Blanpain-Avet et al. [16]. Once the hydraulic and thermal performance of the considered PHEs [17] were implemented in this software, the wall temperatures of the plates at any location in the heat exchanger could be calculated from the inlet temperatures and flow rates of the hot and cold fluids.

The $k-\varepsilon$ turbulence model is adopted to describe the fluid flow in PHE.

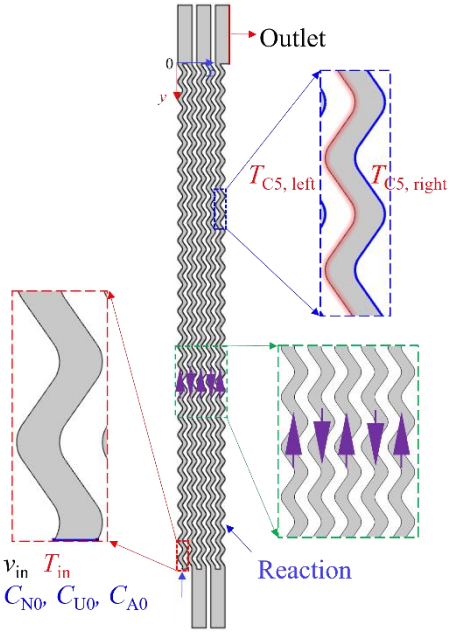

Fig. 2. Initial and boundary conditions of the PHE. The black, blue, and red fonts refer to the momentum transfer, mass transfer, and heat transfer, respectively. The purple arrows in the five channels indicate the product flow direction. v_{in}, T_{in}, C_{N0}, C_{U0}, and C_{A0}, shown in the left enlarged view, are inlet boundary conditions of velocity, temperature, concentration of native BLG, unfolded BLG and aggregated BLG, respectively. The 5th channel with the enlarged view on the right is taken as an example to show the temperature conditions. $T_{C5,\ left}$ and $T_{C5,\ right}$ are the temperature distribution on the left and right side, respectively.

For the denaturation and deposition of whey protein, chemical reactions are used to describe related phenomena. Whey protein enters the PHE at initial concentrations of C_{N0}, C_{U0}, and C_{A0}, after which it is denatured and deposited by heat exchange with hot water. In the bulk reaction, the native BLG forms unfolded BLG as the temperature increases, and the unfolded BLG aggregates to form aggregated BLG, see Eq. (1) (described here with a two-step successive model). The reaction rates of the species are shown in Eq. (2-4), which were reported in several works [1, 14, 18, 19]:

$$\mathrm{N} \xrightarrow{k_U, n_U} \mathrm{U},\ \mathrm{U} \xrightarrow{k_A, n_A} \mathrm{A} \tag{1}$$

$$r_N = k_U C_N^{n_U} \tag{2}$$

$$r_U = k_U C_N^{n_U} - k_A C_U^{n_A} \tag{3}$$

$$r_A = k_A C_U^{n_A} \tag{4}$$

where r_N, r_U and r_A are reaction rates of native BLG, unfolded BLG and aggregated BLG, respectively, with a unit kg/(m^3·s). C_N and C_U are the concentration of native BLG and unfolded BLG, g/L; n denotes the reaction order; k_i is the reaction rate constant, which can be represented by the Arrhenius equation as a function of temperature:

$$k_i = k_{i0} \exp\left(-\frac{E_{a,i}}{RT}\right) \tag{5}$$

where i = U or A are used for the denaturation reaction. k_{i0}, pre-exponential factor, with a unit g^{1-n}L^{n-1}s^{-1}. E_a, activation energy, J/mol; R is universal gas constant, with a value of 8.314 J/(mol·K).

The kinetic parameters of the denaturation reaction at $n_A = n_U = 1.5$ were taken from Khaldi's thesis [19].

The surface reaction can be described as

$$\mathrm{U} \xrightarrow{k_D, n_D} \mathrm{D} \tag{6}$$

With a reaction rate (i.e., deposition rate) of

$$r_D = k_D C_U^{n_D} \tag{7}$$

The surface reaction rate constant k_D (m/s) can also be represented by the Arrhenius equation, as shown in Eq. (5), and for this case, i = D.

ISBN: 978-0-9984188-3-4; Published online www.heatexchanger-fouling.com

The reaction order of the deposition process is n_D = 1.0, which was adopted in several works [13, 14].

Derivation of the surface reaction rate constant k_D

Much of the existing research on fouling formation has applied De Jong's kinetic parameters to estimate the surface reaction rate constant k_D for predicting fouling in whey protein solutions. However, the applicability of these parameters and whether the surface reactions conform to an Arrhenius-like behavior for whey protein solutions remain uncertain. To address this challenge, our approach utilizes preliminary experimental data to establish accurate kinetic parameters for deposit formation. According to the fouling deposit mass and running time of the fouling experiment, k_D can be roughly calculated according to Eq. (7). Where, the deposition rate r_D is determined based on Eq. (8), and C_U is derived from Eqs. (9-10). Eq. (10) was proposed by Tolkach et al. [20]:

$$r_D = \frac{dm_D}{dt \cdot A_e} \quad (8)$$

$$C_U = \alpha \cdot C_S \quad (9)$$

$$\alpha = \exp\left(\frac{\ln(k_U) - \ln(k_A)}{n}\right) \quad (10)$$

where m_D is mass of deposit of one channel, g; A_e is the effective heat exchange area of one channel of PHE, m^2; α denotes the unfolding degree; C_S is the concentration of soluble BLG, g/L.

Fig. 3 shows the variations of ln(k_D) with respect to temperature in the five PHE channels, under three different temperature distributions. These distributions are preliminary and will be further refined in this study.

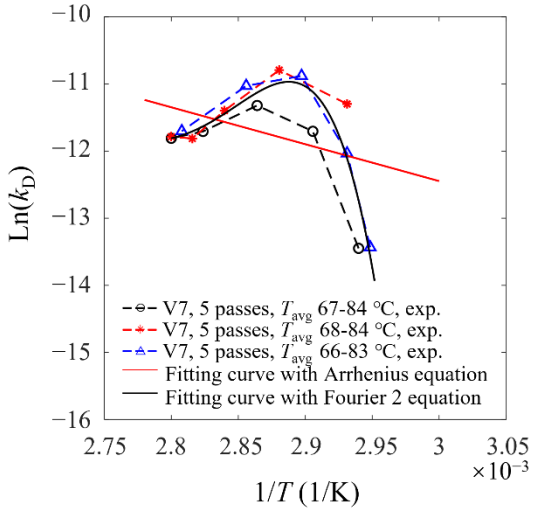

Fig. 3. ln(k_D) changes with the reciprocal of temperature. The dashed lines with circular symbols are the experimental results from Khaldi [19]. The solid lines are fitting curves obtained in two different ways: (i) one equation of the Arrhenius equation (red color in Fig. 3), and (ii) a 2-degree Fourier equation (black color in Fig. 3).

With the hypothesis assumed (n_D = 1.0 and the trend of ln(k_D) change with time), it can be clearly shown that $\ln(k_D)$ is far from following an Arrhenius law, $\ln(k_D) = \ln(k_{D0}) - E_a/(RT)$.

Consequently, we have decided to describe the dependence of the kinetic reaction parameters on temperature by Eq. (11).

$$\ln(k_D) = a_0 + a_1\cos(T \cdot w) + b_1\sin(T \cdot w) + a_2\cos(2T \cdot w) + b_2\sin(2T \cdot w) \quad (11)$$

where $a_0 = -1.08\times10^6$, $a_1 = 1.16\times10^5$, $b_1 = 1.44\times10^6$, $a_2 = 3.57\times10^5$, $b_2 = -5.79\times10^4$, and $w = 5.30\times10^2$.

In this way, kinetic reaction parameters could be obtained for any specific system.

Quantification methods

Based on known k_D values and simulation results (C_U is known), the fouling mass per unit area can be calculated according to Eq's. (7) and (8),

$$m_{D,m^2} = k_D C_U^{n_D} t \quad (12)$$

With k_D from Eq. (11). The average fouling thickness in PHE could be obtained.

$$h_D = \frac{m_{D,m^2}}{\rho_D} \quad (13)$$

where ρ_D is density of fouling deposit, kg/m^3.

RESULTS

According to the above settings, the velocity distribution in the PHE is shown in Fig. 4(a). As we can see, the velocity is greater near the midline, and the velocity of the flowing shadow zone, which is the wavy zone on the outside, is very small. Both the velocity and boundary conditions of the temperature result in the temperature distribution of the PHE, as shown in Fig. 4(b). The overall temperature shows a trend of increasing along the direction of fluid flow, only the temperature of the fifth channel does not seem to conform to this temperature rising trend, which is due to contact of the fifth channel with the lower ambient temperature. Furthermore, a lower velocity in the shadow zone leads to a lower temperature.

ISBN: 978-0-9984188-3-4; Published online www.heatexchanger-fouling.com

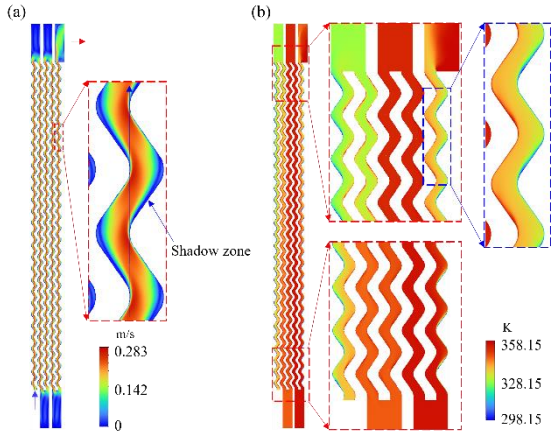

Fig. 4. (a) Velocity distribution, and (b) temperature distribution in PHE. The red and blue dashed boxes are used for enlarging the PHE.

Whey protein denaturation and deposition behavior in PHEs were performed. Fig. 5 illustrates the distribution of different states of the BLG within the PHE. Fig. 5(a), (b), and (c) show the concentrations of native BLG, unfolded BLG and aggregated BLG, respectively. The results for the native BLG showed a decreasing trend along the PHE trajectory, which was as expected. The decreased native BLG was converted to unfolded BLG, as shown in Fig. 5(b). The concentration of unfolded BLG exhibited an increasing trend even if the concentration decreased at the end of PHE when the aggregation reaction in the bulk took off (as shown in Fig. 5(c) and Fig. 6). Notably, through the terminal channel of the PHE, the native BLG was entirely absent, suggesting complete conversion to other states under these processing conditions.

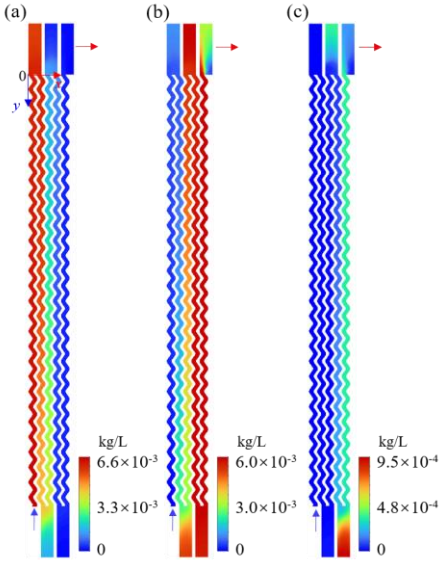

Fig. 5. Concentrations of (a) native BLG, (b) unfolded BLG, and (c) aggregated BLG. The arrows denote the flow direction, the blue arrow denotes the inlet, and the red color denotes the outlet.

The quantitative trend of the BLG constitution is shown in the left coordinate in Fig. 6.

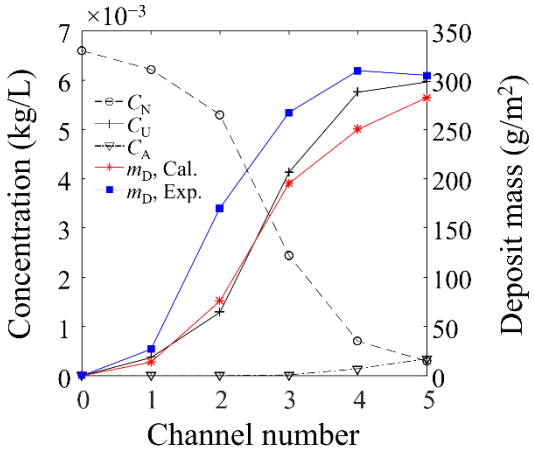

Fig. 6. Concentrations of BLG and the mass deposit along the PHE channels after 2 h.

Based on Eq. (11), the concentration results are shown on the left ordinate axis in Fig. 6. The native BLG showed a decreasing trend, while the unfolding BLG increased until it reached a plateau, when the population of BLG aggregates became significant. This is exactly the same as the phenomenon shown in Fig. 5. According to Eq. (12), the distribution of fouling mass along channels could be obtained. Along the flow direction from the inlet, the calculated fouling mass (red color, right ordinate axis in Fig. 6) increases and then increases more slowly, which is consistent with the overall trend of the unfolded BLG (black solid line, left ordinate axis in Fig. 6). The simulated relationship is determined by the quantitative description between the fouling mass and unfolded BLG (see Eq. (12)). Thus, the overall distributions of the concentrations of the unfolded BLG and deposit mass are expected to evolve similarly. A comparison with the experimental data (blue color, right ordinate axis in Fig. 6) reveals that the simulated fouling mass is in agreement with the experimental mass even if it is slightly underestimated. (1) Fouling is underestimated in the shadow zone and (2) mineral sedimentation occurs during experiment is one possible reason for this underestimation in simulation. Another reason is that (3) the temperature profile imposed is underestimated because the temperature profile is calculated without considering fouling (for a clean plate), and the real temperature profile is slightly higher during the course of fouling. Indeed, to maintain the outlet temperature of the product during fouling run, the flow rate of hot water has to increase to compensate for insulation due to fouling mass deposits. Even if care has been taken, it cannot be excluded that small differences arise from the model of surface deposition (constant estimation and choice of reaction order).

ISBN: 978-0-9984188-3-4; Published online www.heatexchanger-fouling.com

The distribution of fouling deposits along the channel was calculated to examine their impact on the geometry of the system, which will further impact fluid flow and thermal effectiveness. As shown in Fig. 7, there is a notable correlation between the fouling layer thickness and the channel position. For the first channel, there is almost no deposit (a small increase in the fluid flow direction). For channel 2 and channel 3, the fouling thickness increased significantly, while the deposition exhibited almost a steady state for the last two channels. The unfolding BLG reaches the greatest thickness in the latter part of the fifth channel at approximately 0.35 mm (not considering the unsteady area at the end of the fifth channel), which reaches 17.5% of the distance between the two plates (4 mm). Interestingly, the evolution of fouling thickness was linear, but the increase was not monotonic along each channel. For example, channel 2 and channel 3 indicate drastic increases in deposit thickness. This is not the case for the three other channels where the evolution of fouling thickness changes is less important (channels 1, 4 and 5).

This counterintuitive phenomenon shows that the dynamics of deposit formation cannot be reduced to a temperature-dependent reaction. Instead, they are significantly influenced by the presence of unfolded BLG, which seems to act as a precursor to fouling, and the concentration of unfolded BLG is also strongly affected by the competition between the probability of aggregation in the bulk and surface deposition.

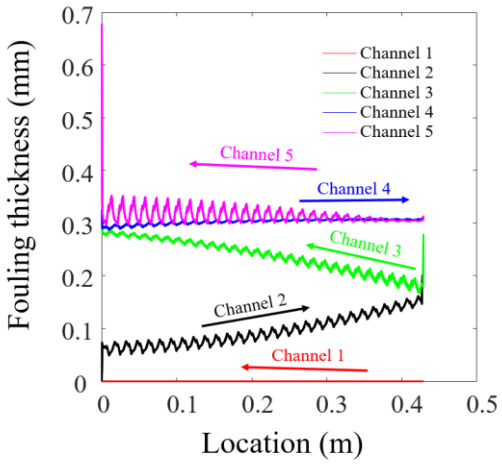

Fig. 7. Fouling deposit thickness along the PHE channel after 2 h.

The forthcoming phase of our research will be dedicated to rigorously testing the proposed models against additional fouling scenarios beyond those used to set up the model. This will involve applying varying denaturation kinetics and exploring a broader spectrum of heat treatment conditions to validate the robustness and applicability of the models. Specifically, we aimed to verify whether the data-driven model, designed for whey protein solutions with calcium, maintains its predictive accuracy beyond the range for which it was originally established.

To achieve this goal, we will undertake comprehensive measurements of deposit mass and thickness throughout the PHE. These evaluations will serve as a benchmark for assessing the model's extrapolative power and its potential as a generalizable tool for the dairy industry.

CONCLUSION

In this study, a two-dimensional model of a PHE, that accurately captures the real temperature distribution within the system, was developed. To investigate the fouling deposition process in the channel, the fouling kinetic parameters suitable for this system were derived from the experimental data. A novel approach for modeling the kinetics of deposit formation has been introduced, streamlining the prediction of fouling deposition. Furthermore, the distribution of fouling in different channels can be visualized by calculating the localized fouling thickness with time.

This approach allows for a more direct reflection of the interaction between fouling and the bulk liquid, and it could serve as a reliable tool for predicting lactoserum fouling, facilitating a comprehensive understanding of the mechanism of milk fouling formation and thus offering valuable insights that could lead to more efficient and cost-effective strategies for managing fouling in dairy processing equipment.

NOMENCLATURE

Symbol

a_0, a_1, b_1, a_2, b_2, w	Fitting parameters
A	Aggregated BLG
A_e	Effective heat exchange area of PHE, m^2
C	Concentration, g/L
D	Deposited BLG
E_a	Active energy, J/mol
h_D	Thickness of fouling deposit, m
k_D	Surface reaction rate constant, m/s
k_i	Reaction rate constant, $g^{1-n}L^{n-1}s^{-1}$
k_0	Pre-exponential factor, $g^{1-n}L^{n-1}s^{-1}$
m_D	Mass of deposit, g
m_{D,m^2}	Mass of deposit per unit area, g/m^2
n	Reaction order
N	Native BLG
t	Time, s
T_{in}	Inlet temperature, K
r_i	Reaction rate, $kg/(m^3 \cdot s)$
r_D	Deposition rate, $kg/(m^2 \cdot s)$
R	Universal gas constant, J/(mol·K)
U	Unfolded BLG
v_{in}	Inlet velocity, m/s

Greek Letters

ISBN: 978-0-9984188-3-4; Published online www.heatexchanger-fouling.com

α	Unfolding degree
ρ_D	Density of fouling deposit, kg/m^3

Subscript

C	Channel
i	U or A
left	Left side
right	Right side
S	Soluble BLG
0	Initial

ACKNOWLEDGEMENTS

We are grateful for the financial support from the National Natural Science Foundation of China (21978184), the China Scholarship Council - Joint Programme for Innovative Talent Training (Functional Food Engineering for Nutrition and Health), the International Associated Laboratory - FOODPRINT (Soochow University (China) - INRAE and Institut Agro (France)), and the "Priority Academic Program Development (PAPD) of Jiangsu Higher Education Institutions".

REFERENCES

[1] Liu, W., *Role of casein micelle on the thermal denaturation of whey protein solutions and fouling mechanisms*, Lille University, 2022.

[2] Van Asselt, A.J., Vissers, M.M., Smit, F., De Jong, P., Inline control of fouling, *Proceedings of Heat Exchanger Fouling and Cleaning—Challenges and Opportunities, Engineering Conferences International*, Irsee, Germany, June 2005

[3] Petit, J., Herbig, A.L., Moreau, A., Delaplace, G., Influence of calcium on beta-lactoglobulin denaturation kinetics: Implications in unfolding and aggregation mechanisms, *J. Dairy Sci.* 94, 5794-5810, 2011.

[4] Qi, X.L., Brownlow, S., Holt, C., Sellers, P., Thermal denaturation of β-lactoglobulin: effect of protein concentration at pH 6.75 and 8.05, *Biochim. Biophys. Acta* 1248, 43-49, 1995.

[5] Liu, W., Feng, Y., Delaplace, G., Andre, C., Chen, X.D., Effect of calcium on the reversible and irreversible thermal denaturation pathway of beta-lactoglobulin, *Food Hydrocolloids* 133, 107943, 2022.

[6] Gu, Y., Bouvier, L., Tonda, A., Delaplace, G., A mathematical model for the prediction of the whey protein fouling mass in a pilot scale plate heat exchanger, *Food Control* 106, 106729, 2019.

[7] Hu, Z., He, X., Huang, T., Yang, M., Qin, G., Full-scale research on the fluid flow and heat transfer of low-flux chevron-type plate heat exchangers under the equal-velocity condition, *Numerical Heat Transfer Part a-Applications* 70, 887-901, 2016.

[8] Grijspeerdt, K., Hazarika, B., Vucinic, D., Application of computational fluid dynamics to model the hydrodynamics of plate heat exchangers for milk processing, *J. Food Eng.* 57, 237-242, 2003.

[9] Choi, W., Jun, S., Nguyen, L.T., Rungraeng, N., Yi, H., Balasubramanian, S., Puri, V.M., Lee, J., 3-D milk fouling modeling of plate heat exchangers with different surface finishes using computational fluid dynamics codes, *J. Food Process Eng.* 36, 439-449, 2013.

[10] Khaldi, M., Ronse, G., André, C., Blanpain-Avet, P., Bouvier, L., Six, T., Bornaz, S., Croguennec, T., Jeantet, R., Delaplace, G., Denaturation kinetics of whey protein isolate solutions and fouling mass distribution in a plate heat exchanger, *International Journal of Chemical Engineering* 2015, 1-10, 2015.

[11] Bouvier, L., Moreau, A., Ronse, G., Six, T., Petit, J., Delaplace, G., A CFD model as a tool to simulate β-lactoglobulin heat-induced denaturation and aggregation in a plate heat exchanger, *J. Food Eng.* 136, 56-63, 2014.

[12] Blanpain-Avet, P., Hédoux, A., Guinet, Y., Paccou, L., Petit, J., Six, T., Delaplace, G., Analysis by Raman spectroscopy of the conformational structure of whey proteins constituting fouling deposits during the processing in a heat exchanger, *J. Food Eng.* 110, 86-94, 2012.

[13] Liu, W., Feng, Y., Pan, F., Jeantet, R., Andre, C., Chen, X.D., Delaplace, G., Effect of calcium on the thermal denaturation of whey proteins and subsequent fouling in a benchtop fouling device: An experimental and numerical approach, *Food Bioprod. Process.* 136, 1-13, 2022.

[14] Pan, F., Chen, X.D., Mercade-Prieto, R., Xiao, J., Numerical simulation of milk fouling: Taking fouling layer domain and localized surface reaction kinetics into account, *Chem. Eng. Sci.* 197, 306-316, 2019.

[15] De Jong, P., *Modelling and optimization of thermal processes in the dairy industry*. The Netherlands, Delft Univ. of Tech., 1996.

[16] Blanpain-Avet, P., Andre, C., Khaldi, M., Bouvier, L., Petit, J., Six, T., Jeantet, R., Croguennec, T., Delaplace, G., Predicting the distribution of whey protein fouling in a plate heat exchanger using the kinetic parameters of the thermal denaturation reaction of beta-lactoglobulin and the bulk temperature profiles, *J. Dairy Sci.* 99, 9611-9630, 2016.

[17] Leuliet, J.C., *Hydraulic and thermal behavior of heat exchangers(interchanges) with plates(patches) handling products not - newtoniens*, France, Nancy I University, 1988.

[18] de Jong, P., Impact and control of fouling in milk processing, *Trends Food Sci. Technol.* 8, 401-405, 1997.

[19] Khaldi, M., *Relationship between milk derivatives' physical chemistry and their ability to foul during thermomechanical treatments in heat exchanger*, Lille University, 2016.

[20] Tolkach, A., Kulozik, U., Reaction kinetic pathway of reversible and irreversible thermal denaturation of β-lactoglobulin, *Le Lait* 87, 301-315, 2007.

ISBN: 978-0-9984188-3-4; Published online www.heatexchanger-fouling.com